

HOW DO Z AND ATOLL X-RAY BINARIES DIFFER?

MICHAEL P. MUNO, RONALD A. REMILLARD, AND DEEPTO CHAKRABARTY¹

Department of Physics and Center for Space Research, Massachusetts Institute of Technology, Cambridge, MA 02139

muno,rr,deepto@space.mit.edu

Draft version May 28, 2018

ABSTRACT

Low-mass X-ray binaries containing weakly magnetized neutron stars may be divided into two classes, Z and atoll sources, based upon correlations between their X-ray timing properties and the patterns which they trace in plots of two X-ray colors. In this paper, we examine color-color diagrams of eight atoll sources and four Z sources using data from the *Rossi X-ray Timing Explorer*. The five-year span of data we have examined is significantly longer than those of previous studies. We find that the previous clear distinction between color-color diagrams from atoll and Z sources is an artifact of incomplete sampling, as those atoll sources which are sampled over a wide dynamic range in intensity ($F_{\max}/F_{\min} \gtrsim 80$) trace three-branched color-color patterns similar to the tracks for which Z sources are named. However, atoll sources trace this pattern over a larger range of luminosity and on much longer time scales than do Z sources, and exhibit much harder spectra when they are faint, which argues against any simple unification scheme for the two classes of source.

Subject headings: stars: neutron — X-rays: stars

1. INTRODUCTION

Low-mass X-ray binaries (LMXBs) containing weakly-magnetized neutron stars may be divided into two classes, Z and atoll sources, based upon correlations between their spectral colors and Fourier timing properties at X-ray wavelengths (Hasinger & van der Klis 1989). Plots of a “hard” color against a “soft” color from Z sources usually form a Z shape that is traced on time scales of hours to days (bottom panels of Figure 1). Plots from atoll sources often resemble a band of points at constant hard color, with “islands” of points appearing on time scales of weeks and months (see 4U 1820-303 in Figure 1). Power spectra from both types of sources may be described with similar broad-band noise components, but Z sources exhibit strong (up to 10% rms) quasi-periodic oscillations (QPOs) between 1–60 Hz, while atoll sources do not (but see Wijnands & van der Klis 1999; Psaltis, Belloni, & van der Klis 1999). The exact causes of the spectral and timing variability is still unknown, but it is thought that the differences between the two classes result from a higher rate of mass transfer in Z sources than atoll sources (see van der Klis 1995, for a review).

In this *Letter*, we examine the spectral changes that occur in Z and atoll sources, using the public archive of observations taken with the Proportional Counter Array (PCA; Jahoda et al. 1996) aboard the *Rossi X-ray Timing Explorer* (*RXTE*). This unprecedented database of PCA observations, which samples the spectral variability of LMXBs on time scales from seconds to years, allows us to present a complete picture of the X-ray color changes that occur in these systems.

2. DATA ANALYSIS

We have obtained all of the publicly available *RXTE* PCA data as of 2001 September (along with some pro-

prietary data) for twelve neutron star LMXBs (Table 1). Seven of these LMXBs have been previously classified as atoll sources and four as Z sources (van der Klis 1995; Reig et al. 2000), while one (GS 1826–238) is probably an atoll source since it prolifically produces thermonuclear X-ray bursts (Ubertini et al. 1999; van der Klis 1995). The public archive of pointed observations of these sources contains many dozens of observations between 3000 to 30,000 seconds long, spanning over five years.

We have examined data with 128 energy channels between 2–60 keV and 16 s time resolution from the PCA, and daily flux histories from the *RXTE* All-Sky Monitor (ASM; Levine et al. 1996). We list some basic properties of the sources in Table 1. The variability is defined as the ratio of the maximum to minimum count rate observed with the PCA between 2–18 keV, and is a lower limit to the true value. This sample of sources spans a factor of 100 in average luminosity, and a factor of 1000 in variability.

We have defined hard and soft colors as the ratio of the background-subtracted detector counts in the (3.6–5.0)/(2.2–3.6) keV and the (8.6–18.0)/(5.0–8.6) keV energy bands, respectively, to produce color-color and color-intensity diagrams (Figures 1–3). We have used 64 s integrations to calculate the colors when the source intensity is above 100 counts s⁻¹, and 256 s integrations otherwise. Gain changes in the five individual proportional counter units (PCUs) of the PCA over the course of the mission cause systematic variation in these count rates (e.g., Homan et al. 2001, for a more detailed discussion). Therefore, we have normalized the count rates from the Crab Nebula in each PCU to constant values for each energy band (totaling 2440 counts s⁻¹ PCU⁻¹ in the 2.2–18.0 keV band) using linear trends. When this correction is applied, the hard and soft colors from the Crab Nebula have values of 1.358 and 0.679, with standard deviations of only 0.5% and 0.1% respectively.

¹ Alfred P. Sloan Research Fellow

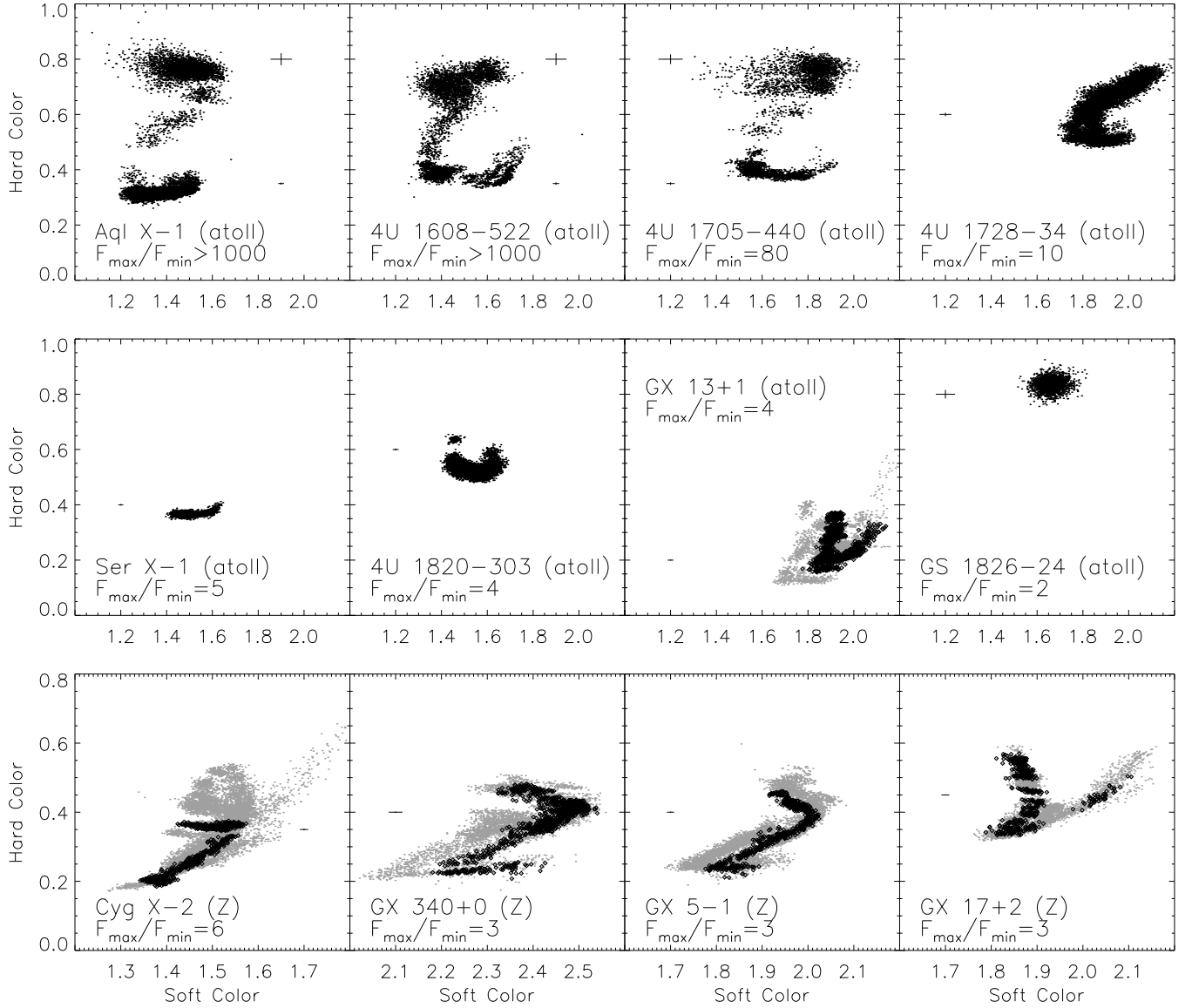


FIG. 1.— Color-color diagrams from five years of pointed *RXTE* PCA observations. Typical uncertainties are indicated to the side of the data. The atoll sources that vary by the widest range in intensity trace Z-shaped tracks, similar to those of Z sources. The remaining atoll sources trace portions of this complete track. The Z sources differ from the atoll sources in that they tend to be softer, and they trace their full range of spectral variability on time scales of days and with smaller intensity variations. GX 13+1 is unusual, in that it has been previously classified as an atoll source, yet its color-color diagram resembles that of the Z source GX 17+2 more than any other source. We have highlighted data spanning twenty days for sources that trace a complete pattern in their X-ray colors on day-long time scales: MJD 50980–51000 for GX 13+1, MJD 50600–50620 in GX 340+0, MJD 50990–51010 for Cyg X-2, and MJD 50530–50550 for GX 17+2. Each time interval contains between 4–17 observations.

3. RESULTS

We plot the color-color diagrams in Figure 1. The most striking aspect of Figure 1 is that a Z-shape is formed in color-color diagrams from the atoll sources that vary by the widest range in X-ray intensity: Aql X-1, 4U 1608–522, and 4U 1705–44 (Table 1). It has long been suspected that the complete color-color diagram from atoll sources forms a Z-shape (e.g. Langmeier, Hasigner, & Trümper 1989), but this is the first time that atoll sources have been adequately sampled over a wide enough range of luminosity to observe this pattern directly. Several more sources that vary by no more than a factor of 10 in X-ray intensity ap-

pear to form portions of this pattern. 4U 1820–303 and 4U 1728–34 in Figure 1 exhibit only the bottom and diagonal portions of this pattern. Ser X-1 exhibits only the bottom portion, and GS 1826–238 only the top (Figure 1).

The tracks from the Z sources Cyg X-2, GX 17+2, GX 5–1, and GX 340+0 (Figure 1) are unmistakably Z-shaped, but are somewhat different from those of the atoll sources. In general, Z sources are softer than atoll sources. Moreover, the traditional Z sources trace out a full track on time scales as short as a day, while atoll sources form their color-color diagrams on much longer time scales of 30–100 days. We have highlighted using darker symbols data spanning 20 days for the sources which trace their

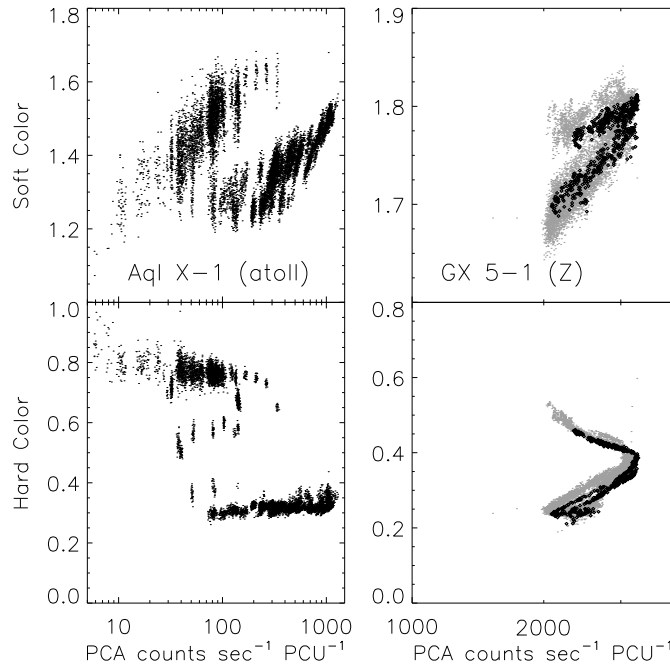


FIG. 2.— Plots of hard and soft color versus the PCA count rate between 2–18 keV for Aql X-1 (left) and GX 5-1 (right). Notice that narrower correlations between color and count rate are observed on time scales of a day in Aql X-1. For GX 5-1, we have highlighted observations spanning 20 days to account for global shifts in the position of the colors on longer time scales, as in Figure 1.

Z on short time scales in Figure 1, in order to allow an easy comparison between the short and long-term spectral variability. As has been previously noted, the width of the track perpendicular to the direction of motion is much smaller in traditional Z sources than in atoll sources when observed on time scales of days (e.g. van der Klis 1995). On the five-year time scales of Figure 1, both the Z and atoll sources exhibit 10–20% variations in the colors perpendicular to the direction of motion that traces the Z (e.g. Kuulkers et al. 1994).

It is interesting to note that the color-color diagram of GX 13+1 in Figure 1 resembles that of the Z source GX 17+2 more than those of the other atoll sources. Although GX 13+1 was classified an atoll source because it lacked strong QPOs (Hasinger & van der Klis 1989), *RXTE* observations have revealed weak QPOs similar to those of Z sources (Homan et al. 1998), and several observations have revealed similarities between the X-ray (Schulz et al. 1989) and IR (Bandyopadhyay et al. 1999) spectra of GX 13+1 and other Z sources. GX 13+1 appears to exhibit both Z and atoll properties, and may prove important for understanding what causes the distinctions between the two classes of source.

We next examine how these colors evolve versus intensity and, for the atoll sources, versus time. In Figure 2 we have plotted the hard and soft color as a function of the 2–18 keV PCA count rates for the atoll source Aql X-1 and the Z source GX 5-1. In Figure 3 we have plotted the X-ray colors and the 2–12 keV X-ray intensity from the *RXTE* ASM from the atoll source 4U 1705–440 over a span of 200 days. It is well-known that Z sources trace their color-color diagrams smoothly with time in less than a day (e.g. Kuulkers et al. 1994; van der Klis 1995). These data are the best-sampled examples from the LMXBs in

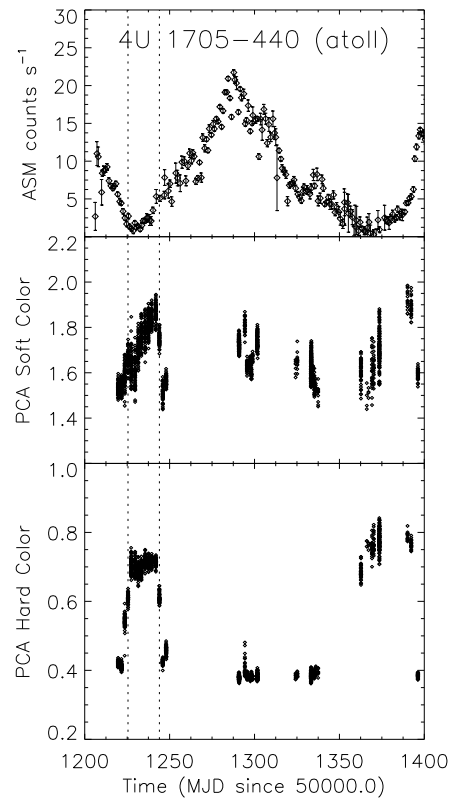


FIG. 3.— The evolution of the X-ray intensity and colors as a function of time for 4U 1705–440. *Top Panel*: X-ray intensity measured with the ASM (2–12 keV). *Middle and Bottom Panels*: Soft and hard X-ray colors. The diagonal portion of the color-color diagram appears as the rapid change in hard color (see dashed lines), which occurs at a higher count rate in the rise of an outburst than in the decay.

Table 1.

Figures 2 and 3 indicate that atoll sources also trace their Z-shaped track smoothly. The horizontal portion at the top of the color-color track of the atoll sources (with a hard color of about 0.8 in Figure 1) is traced from left to right as the intensity increases by more than a factor of 10. For Aql X-1 and 4U 1608-522, it is traced on time scales of days to months as the source rises from (or decays to) below the PCA detection threshold, with a factor of 250 change in intensity. On the other hand, GS 1826–34 has remained in a similar faint and hard state for the six years of *RXTE* monitoring.

The diagonal branch is traced on time scales of days, and only has been sampled well in time in a few instances (e.g. Figure 3). As an atoll source moves down along the diagonal portion of the color-color track, the count rate usually increases by a factor of 2 (and vice versa; see Figure 3). However, during a recent unusual outburst of Aql X-1 (Bailyn et al. 2001) the count rate decreased by a factor of 2 while moving down along the diagonal branch (not shown). The overall intensity on this branch is higher in the rise of an outburst ($100\text{--}300\text{ counts s}^{-1}\text{ PCU}^{-1}$ for Aql X-1 in Figure 2) than in the decay ($<100\text{ counts s}^{-1}\text{ PCU}^{-1}$ for Aql X-1; see also Figure 3). Since the soft color increases with intensity along the top branch (Figure 2), the value of soft color at which the diagonal and top branches connect also could be smaller in the rise of an outburst than in the decay, as may be seen by compar-

ing the soft colors near the dates indicated by dashed lines in Figure 3. Similar hysteresis has been observed from transient LMXBs containing black holes (Miyamoto et al. 1995).

The bottom portion of the color-color track from the atoll sources (hard color of 0.3) is traced from left to right as the count rate increases once again by a factor of 10 (from 70–1500 counts s^{-1} PCU $^{-1}$ in Figure 2). This branch is traced on time scales of days to weeks in the transient sources, while Ser X-1 has remained in this soft state throughout the *RXTE* mission.

The color-color diagrams of Z sources are known to be traced smoothly, without jumping between branches, but the color changes are not accompanied by large variations in the X-ray intensity (right panels of Figure 2). The top portion of the color-color track from GX 5–1 (hard color of 0.4 in Figure 1) is traced as the count rate increases by 70% (Figure 2). On the diagonal portion of the color-color track of GX 5–1, the count rate returns to its lowest values. In atoll sources, the intensity is nearly constant. On the bottom of the color-color track, the count rate of GX 5–1 steadily increases yet again by 70%. The intensity from other Z sources changes by up to a factor of three on this track (e.g., Homan et al. 2001, for GX 17+2).

The hardness-intensity diagram of the atoll source Aql X-1 in Figure 2 also reveals important sub-structure on short time scales that is common to all of the atoll sources in Table 1. This structure is most evident in the plot of soft color against count rate, where narrow, parallel tracks are traced by observations within single days. At low intensities (less than 200 counts s^{-1} PCU $^{-1}$), the soft color varies as the count rate remains nearly constant, while at the highest intensities, the soft color and count rate both increase significantly together. On the color-color diagram in Figure 1, these daily tracks are generally aligned perpendicular to motion along the Z, and thus broaden the color-color tracks of the atoll sources. In contrast, the parallel tracks from the Z sources are formed when the entire Z shifts (van der Klis 2000).

4. DISCUSSION

We have demonstrated that the color-color diagrams of both Z and atoll sources have similar three-branched shapes (Figures 1), but that the range of X-ray intensity and the time scale over which the diagrams are traced are one to two orders of magnitude larger in the atoll sources (Figures 2 and 3). We note that similar conclusions have been reported independently by Gierliński & Done (2002). There are also significant spectral differences between the two classes of source (Schulz et al. 1989; Christian & Swank 1997; Barret et al. 2000). The spectra of Z sources are always soft, and can be described by the sum of a cool (1 keV) black body and Comptonized emission from warm (5 keV) optically thick electrons (e.g., Christian & Swank 1997; Di Salvo et al. 2000). Spectral changes along the

Z are quite subtle (e.g., Schulz et al. 1989). In contrast, changes in the energy spectra of atoll sources are dramatic. While soft energy spectra resembling those of Z sources are characteristic of atoll sources at the bottom of their color-color diagrams (e.g., Oosterbroek et al. 2001, for Ser X-1), a hard state with a $\Gamma \approx 1.8$ power-law energy spectrum between 2–100 keV occurs at the top of this diagram when the sources are faint (e.g., Barret et al. 2000, for GS 1826–238). Such a hard spectrum is not observed from Z sources, probably because they are not observed at low luminosities (Table 1 and Figure 2).

Recent work has suggested that the timing properties of Z and atoll sources also may have interesting similarities. It has long been suggested that the broad-band noise in power spectra of Z and atoll sources can probably be described by similar components (van der Klis 1995), and detailed studies of *RXTE* data have shown that the frequencies of QPOs and band-limited noise exhibit similar correlations in both types of sources (Wijnands & van der Klis 1999; Psaltis et al. 1999). However, whether the timing properties are correlated with the branches of the color-color diagrams in a similar manner in each class of source remains to be investigated.

The timing properties of neutron star LMXBs eventually may allow us to understand what drives the spectral variability. Several studies have found that the kHz QPO frequencies are well-correlated with position on the color-color diagram in both Z (e.g., Homan et al. 2001) and atoll (e.g., van Straaten et al. 2001) sources. Examining Figure 2, the short-term correlations between the colors and PCA count rate are extremely similar to the “parallel tracks” observed in comparisons of the frequencies of kilohertz quasi-periodic oscillations (kHz QPO) with the PCA count rate (van der Klis 2000, 2001). The parallel tracks are observed from kHz QPOs both in studies of individual sources (Méndez et al. 1999), and in comparing the frequencies of QPOs from Z and atoll sources that span a wide range of luminosity (Ford et al. 2000). Based upon these parallel tracks, van der Klis (2001) has suggested that the kHz QPO frequencies are determined by a feedback process that is sensitive to deviations in the accretion rate about its value averaged over a few days. Further work is needed to determine whether the same feedback mechanism can operate to produce spectral variations in both Z and atoll sources, on widely different time scales and over ranges in luminosity that differ by factors of 100.

We are grateful for questions and comments from Michiel van der Klis and Erik Kuulkers that helped in clarifying these results. This work was supported by NASA, under contract NAS 5-30612 and grant NAG 5-9184, and has made use of data obtained from the High Energy Astrophysics Science Archive Research Center (HEASARC), provided by NASA’s Goddard Space Flight Center

REFERENCES

Bailyn, C., Tourtellotte, S., Walkowicz, L., Gonzalez, D., & Espinoza, J. 2001, IAUC 7671
 Barret, D., Olive, J. F., Boirin, L., Done, C., Skinner, G. K., & Grindlay, J. E. 2000, ApJ, 533, 329
 Bandyopadhyay, R. M., Shahbaz, T., Charles, P. A., & Naylor, T. 1999, MNRAS, 306, 417
 Christian, D. J. & Swank, J. H. 1997, ApJS, 109, 177
 Di Salvo, T. et al. 2000, ApJ, 544, L119

Ford, E. C., van der Klis, M., Méndez, M., Wijnands, R., Homan, J., Jonker, P. G., & van Paradijs, J. 2000, ApJ, 537, 368

Gierliński, M. & Done, C. 2002, MNRAS submitted, astro-ph/0111378

Jahoda, K., Swank, J. H., Giles, A. B., Stark, M. J., Strohmayer, T., Zhang, W., & Morgan, E. H. 1996, in Proc. SPIE 2808, EUV, X-Ray, and Gamma-Ray Instrumentation for Astronomy VII, ed. O. H. Siegmund & M. A. Gumm (Bellingham: SPIE), 59

Hasinger, G., & van der Klis, M. 1989, A&A, 225, 79

Homan, J., van der Klis, M., Wijnands, R., Vaughan, B., & Kuulkers, E. 1998, ApJ, 499, L41

Homan, J., van der Klis, M., Jonker, P. G., Wijnands, R., Kuulkers, E., Méndez, M., & Lewin, W. H. G. 2001, astro-ph/0104323

in 't Zand, J. M. M., Heise, J., Kuulkers, E., Bazzano, A., Cocchi, M., & Ubertini, P. 1999, A&A, 347, 891

Kuulkers, E., van der Klis, M., Oosterbroek, T., Asai, K., Dotaini, T., van Paradijs, J., & Lewin, W. H. G. 1994, A&A, 289, 795

Langmeier, A., Hasinger, G., & Trümper, J. 1989, ApJ, 340, L21

Levine, A. M., Bradt, H., Cui, W., Jernigan, J. G., Morgan, E. H., Remillard, R., Shirey, R. E., & Smith, D. A. 1996, ApJ, 469, L33

Méndez, M., van der Klis, M., Ford, E. C., Wijnands, R., & van Paradijs, J. 1999, ApJ, 511, L49

Miyamoto, S., Kitamoto, S., Hayashida, K., & Egoshi, W. 1995, ApJ, 442, L13

Oosterbroek, T., Barret, D., Guainazzi, M., & Ford, E. C. 2001, A&A, 366, 138

Psaltis, D., Belloni, T., & van der Klis, M. 1999, ApJ, 520, 262

Reig, P., Méndez, M., van der Klis, M., & Ford, E. C. 2000, ApJ, 530, 916

Schulz, N. S., Hasinger, G., & Trümper, J. 1989, ApJ, 225, 48

Shirey, R. E., Bradt, H. V. D., Levine, A. M. 1999, ApJ, 517, 472

Ubertini, P., Bazzano, A., Cocchi, M., Natalucci, L., Heise, J., Muller, J. M., & in 't Zand, J. J. M. 1999, ApJ, 514, L27

van der Klis, M. 1995, in X-Ray Binaries, ed. W. H. G. Lewin, J. van Paradijs, & E. P. J. van den Heuvel (Cambridge U. Press), 252

van der Klis, M. 2000, ARA&A, 38, 717

van der Klis, M. 2001, ApJ, 561, 943

van Straaten, S., van der Klis, M., Kuulkers, E., & Méndez, M. 2001, ApJ, 551, 907

Wijnands, R. & van der Klis, M. 1999, ApJ, 514, 939

TABLE 1
BASIC PROPERTIES OF NEUTRON STAR LMXBs

Source	Type	L_X^b	D^c	N_H^d	Variability ^e
4U 1608-522	A,b	0.1	4	1.5	2000
Aql X-1	A,b	0.1	3	0.5	1000
4U 1705-440	A,b	6	11	1.1	80
4U 1728-34	A,b	0.4	4	1.7	10
Ser X-1	A,b	4	8 ^f	0.5	5
4U 1820-303	A,b	5	7.5	2.6	4
GX 13+1	A,b	5	7 ^f	2.5	4
GS 1826-238	A?,b	0.3	6 ^g	0.5 ^g	2
Cyg X-2	Z,b	16	12	0.3	6
GX 17+2	Z,b	12	8	1.7	3
GX 5-1	Z	18	7	2.5	3
GX 340+0	Z	16	10	5.0	3

^aPrevious classifications of each source. A — atoll source, Z — Z source, b — burster.

^bMean unabsorbed 2-12 keV luminosity in units of 10^{37} erg s⁻¹, inferred from the ASM assuming a $\Gamma = 2.5$ power law spectrum.

^cDistance in kpc, taken from Ford et al. (2000) except where noted

^dAbsorption column in units of 10^{22} cm⁻², taken from Christian & Swank (1995) except where noted.

^e F_{\max}/F_{\min} , 2-18 keV from the PCA.

^fFrom Christian & Swank (1995).

^gFrom in 't Zand et al. (1999).